

Structure–Function Studies of the Lustrin A Polyelectrolyte Domains, RKSY and D4

Brandon A. Wustman,¹ James C. Weaver,² Daniel E. Morse,²
and John Spencer Evans¹

¹Laboratory for Chemical Physics, New York University, New York, USA

²Department of Molecular, Cellular, and Developmental Biology and Materials Research Laboratory, University of California, Santa Barbara, California, USA

The lustrin superfamily represents a unique group of biomineralization proteins localized between layered aragonite mineral plates (i.e., nacre layers) in mollusk shell. These proteins not only exhibit elastomeric behavior within the mineralized matrix, but also adhesion to the aragonite-containing composite layer. One member of the lustrin superfamily, Lustrin A, has been sequenced; the protein is organized into defined, modular sequence domains that are hypothesized to perform separate functions (i.e., force unfolding, mineral adhesion, intermolecular binding) within the Lustrin A protein. Using nuclear magnetic resonance (NMR) and *in vitro* mineralization assays, we investigated structure-function relationships for two Lustrin A putative mineral binding domains, the 30 AA Arg, Lys, Tyr, Ser-rich (RKSY) and the 24 AA Asp-rich (D4) sequence regions domain of the Lustrin A protein. The results indicate that both sequences adopt open, unfolded structures that represent either extended or random coil states. Using geologic calcite overgrowth assays and scanning electron microscopic analyses, we observe that the RKSY polypeptide does not significantly perturb calcium carbonate growth. However, the D4 domain does influence crystal growth in a concentration-dependent manner. Collectively, our data indicate that D4, and not the RKSY domain, exhibits structure-function activity consistent with a mineral binding region.

Keywords Biomineralization, Lustrin A, Polyelectrolyte, Secondary Structure.

INTRODUCTION

Molecular elasticity is associated with a select number of polypeptides and proteins [1–10]. As an example, the lustrins, a protein superfamily localized within layered aragonite mineral plates (i.e., nacre layers) in mollusk shell, have been postulated to

play a role in the enhancement of nacre layer fracture toughness [1, 2]. Recent atomic force microscopic (AFM) pulling studies have demonstrated that the organic layer of the nacre of the red abalone, *Haliotis rufescens*, exhibits a typical sawtooth force-extension curve with hysteretic recovery [2]. The AFM pulling experiments also demonstrated that this lustrin-containing organic matrix layer possessed adhesive interactions, either with the underlying aragonite mineral phase or with other organic matrix components [2]. One particular lustrin protein, Lustrin A (pacific red abalone *H. rufescens*, 116 kDa) is a component of the “insoluble” intercrystalline organic matrix lying between the layers of aragonite tablets [1]. This intercrystalline organic layer also contains β -chitin and β -silk fibroin protein [1, 3]. Using scanning electron microscopic (SEM) and immunolocalization techniques, the Lustrin A protein has been localized to the region between parallel aragonite mineral layers within the nacre; effectively, the protein resides in an organic “strand” that resembles a supramolecular “bungee cord” stretching between adjacent aragonite crystal tablet layers (D. Morse, UCSB, unpublished observations).

Consequently, there is considerable interest in defining the structure-function relationships within the lustrin superfamily and establishing their participation in the shell fracture resistance. We recently investigated the solution-state structure of a 12-residue consensus sequence found near the N-terminal end of the C1–C8 domains within the Lustrin A protein [4]. This consensus sequence, believed to be one of several putative elastic motifs within Lustrin A, was found to adopt a loop structure at pH 7.4 [4]. Not surprisingly, loop regions are believed to behave as entropic springs and are capable of reversible motion or flexibility within proteins [5, 6]. In this report, we continue the use of the model peptide strategy to probe the sequence-structure relationships of modular motifs within Lustrin A. Our present focus is on two domains: the first, a 24-AA Asp-containing domain (-GKGASYDTDADSG-SCNRSPGYLPG- sequence positions

Received 9 November 2001; accepted 15 April 2002.

Address correspondence to Dr. John Spencer Evans, Laboratory for Chemical Physics, NYU, 345 E, 24th St., New York, NY 10010, USA. E-mail: jse@dave-edmunds.dental.nyu.edu

1251–1274), termed “D4”; and the second, an Arg, Lys, Ser, Tyr-rich 30-AA domain (-YRGPIARPRSSRYLAKYLKQGR-SGKRLQKP-, sequence positions 1354–1383), termed “RKS Y” [1]. Our rationale for studying these two domains is that each possesses either putative Ca (II) (D4: Asp) or CO₃²⁻ (RKS Y: Arg, Lys, Tyr, Ser; D4: Arg) binding residues that could permit Lustrin A to “adhere” to mineral surfaces. Using “capped” versions of both peptides, we determined secondary structure preferences for both peptides and explored putative interactions of each peptide with nucleating calcium carbonates in vitro. We find that both peptides adopt an extended and/or “random coil” conformation and that the D4 domain, and not the RKS Y domain, exhibits positive interactions with calcium carbonates in vitro.

EXPERIMENTAL PROCEDURES

Peptide Synthesis and Sample Preparation

Purified, N-acetyl, C-amide capped RKS Y, and D4 polypeptides were synthesized by Dr. Janet Crawford, Yale University HHMI Biopolymer/Keck Biotechnology Resource Laboratory, using an Applied Biosystems 431A Peptide Synthesizer and N^α-L-FMOC-amino acids as described elsewhere [4]. The crude peptides were separately dissolved in deionized distilled water, extracted three times with diethyl ether, and then concentrated and lyophilized. Peptide purification involved C18 reverse phase high performance liquid chromatography (HPLC) column, using 0.1% TFA/water mobile phase and eluting with an 80% acetonitrile/0.1% TFA/water linear gradient. Peptide elution was monitored at 230 nm. Individual HPLC fractions were analyzed using a custom made matrix-assisted laser desorption/ionization-time of-flight (MALDI/TOF) delayed extraction mass spectrometer. The experimental molecular weights for the capped RKS Y and D4 polypeptides were determined to be 3575.6 Da and 2499.96 Da, in agreement with the theoretical molecular weights of 3572.1 Da and 2499.55 Da, respectively. For NMR studies each peptide was dissolved in 1 mM Na₂HPO₄ in deionized distilled water, pH 7.4. NMR samples contained 10% v/v deuterium oxide (99.9% atom D, Cambridge Isotope Labs) and 10 μM d4 TSP. Final peptide concentrations were 2 mM for NMR. For in vitro calcium carbonate assays, the peptides were dissolved in deionized distilled water and the pH was adjusted to 7.0 using NaOH.

NMR Experiments

NMR experiments were performed on a Varian UNITY 500 spectrometer equipped with variable temperature controller and a three-channel (¹³C/¹⁵N/¹H) z-axis PFG 5-mm solution probehead. With the exception of the proton amide temperature shift experiments, all reported NMR experiments were conducted at 278 K to slow down conformational exchange within the peptide. Proton scalar coupling assignments, ³J_{NH-CH α} coupling constants, and short, medium, and long-range nOes were obtained using “excitation sculpting” 2-D PFG homonuclear experiments [7–12]. Using PFG TOCSY or NOESY experiments at 278, 283, 288, 293, and 298 K, amide proton temperature coefficients were determined from the slope of the temperature

versus amide proton chemical shift curves for each residue [4, 13–15].

In Vitro Calcium Carbonate Overgrowth Assays

We employed the geologic calcite fragment overgrowth assay [16, 17] with the following modifications. Briefly, Iceland spar calcite (Ward Scientific) was cleaved into 9–16-mm² fragments that were used immediately. Assays were conducted in borosilicate scintillation vials and were initiated by mixing equal volumes of 12.5 mM CaCl₂ and 12.5 NH₄HCO₃ solutions (3 mL total volume). Microliter volumes of RKS Y, D4, and bovine serum albumin (Pierce Scientific) were added and mixed with reaction media in individual vials; typically a concentration series (6.7 × 10⁻⁹, 1.3 × 10⁻⁸, 3.3 × 10⁻⁸, 1.7 × 10⁻⁷, and 3.3 × 10⁻⁷ M polypeptide) was run in triplicate. Negative controls consisted of reaction media alone. The calcite fragment was introduced into each vial, the vial was sealed and incubated at 15°C for 3 hr. Upon conclusion of the incubation period, calcite fragments were washed 3 times with 3 mL calcium carbonate-saturated methanol, then dried overnight at 37°C to evaporate remaining solvent. Calcite fragments were then mounted on carbon conductive tabs and sputter coated with gold under vacuum/Ar gas to generate a 3–5 nm layer of gold on the mineral surfaces. Imaging of overgrowth films was performed using a JEOL JSM 6300F cold cathode field emission scanning electron microscope, operating at 5 kV.

RESULTS AND DISCUSSION

NMR Secondary Structure Analyses of D4 and RKS Y

Figures 1 and 2 list the sequential intra- and interresidue nOes, nOe ratios, ³J_{NH-CH α} , coupling constants, and amide temperature shift coefficients (ATC) for RKS Y and D4, respectively. Using PFG-NOESY and ROESY experiments (50 ms to 200 ms mixing times) we were unable to detect sequential d_{NN(i,i+1)}, medium or long-range backbone nOes, and for some residues for either peptide; in addition, some intraresidue d _{α (i,i)} nOes were not observed. The absence of intra- and interresidue nOes also have been noted in conformationally labile random coil states and in extended peptide structures [19–21]. The presence of extended or random coil structure is also confirmed by calculation of nOe intensity ratios [α N(i, i + 1)/ α N(i, i)] (Figures 1 and 2). A value of 2.3 is predicted for the population-weighted random coil model, whereas values >4 are predicted for β -strand [19, 22]. For RKS Y, with the exception of the terminal Y1-R2 region, the obtained nearest-neighbor residue pairs possess nOe ratios >2.3, consistent with the presence of extended structure in these regions [22]. By comparison, for D4, the obtained nOe ratios are smaller, indicating a stronger preference for random coil structure in this sequence.

It has been shown that random coil or extended peptides exhibit amide temperature shift coefficients in the range of –6.6––9.0 ppb/K in aqueous solution [13–15]. For both D4 and RKS Y, we found that the temperature coefficients varied from –6.0 to –9.4 ppb/K (Figures 1 and 2), indicating both peptides exist

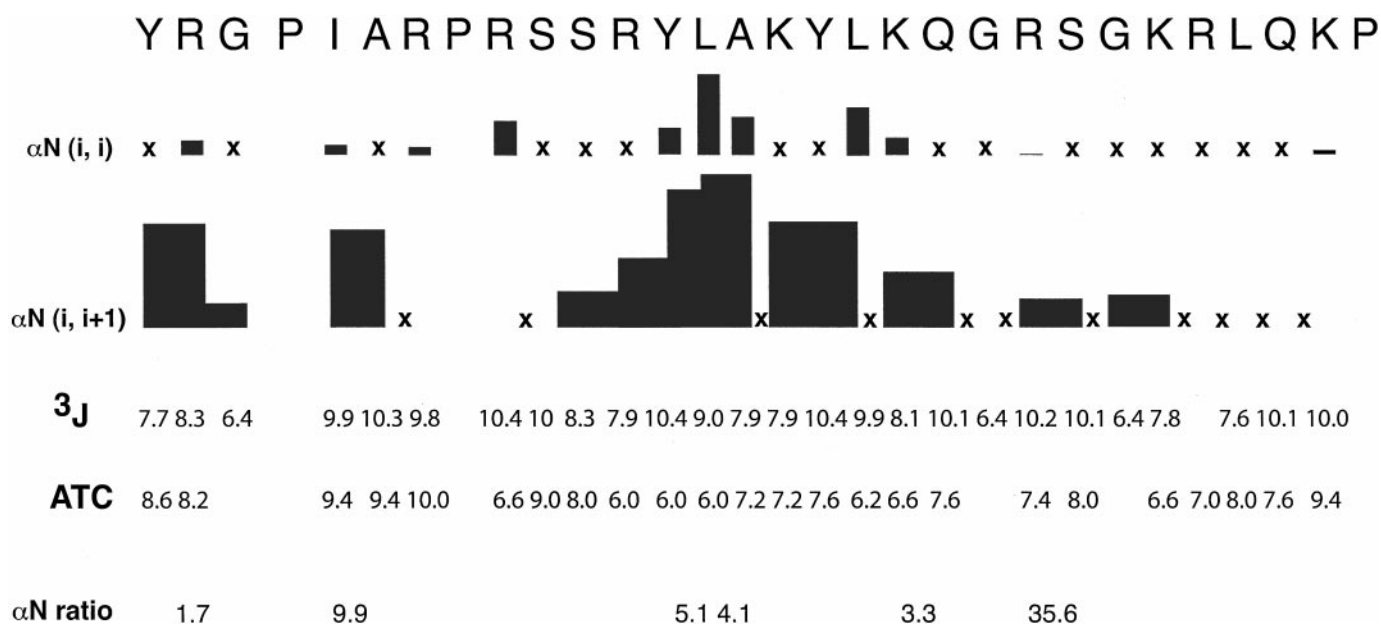


Figure 1. Summary of NMR parameters for Lustrin A RKSYS peptide in 1 mM Na₂HPO₄, 90% water/10% D₂O, 278 K pH 7.4. The summary includes interresidue sequential CH _{α} ,residue “i” to NH _{α} ,residue “i+1” nOes [denoted as $\alpha N(i, i + 1)$], presented as contiguous bars for corresponding interresidue proton pairs] and intrasidue CH _{α} ,residue “i” to NH _{α} ,residue “i” nOe’s [denoted as $\alpha N(i, i)$]. The histogram bar heights reflect the cross-peak intensities of corresponding nOes for each residue or residue pair, determined via integration of the NOESY or ROESY spectra. The αN ratio denotes the ratio of interresidue $\alpha N(i, i + 1)$ nOe cross-peak intensities to intrasidue $\alpha N(i, i)$ cross-peak intensities, determined via cross-peak integration from the spectra. “x” denotes observed nOe but due to cross-peak overlap, relative intensities could not be integrated. Figure 1 also presents 3J couplings (Hz) and amide temperature shift coefficients (ATC, in ppb/K). N/A = not available.

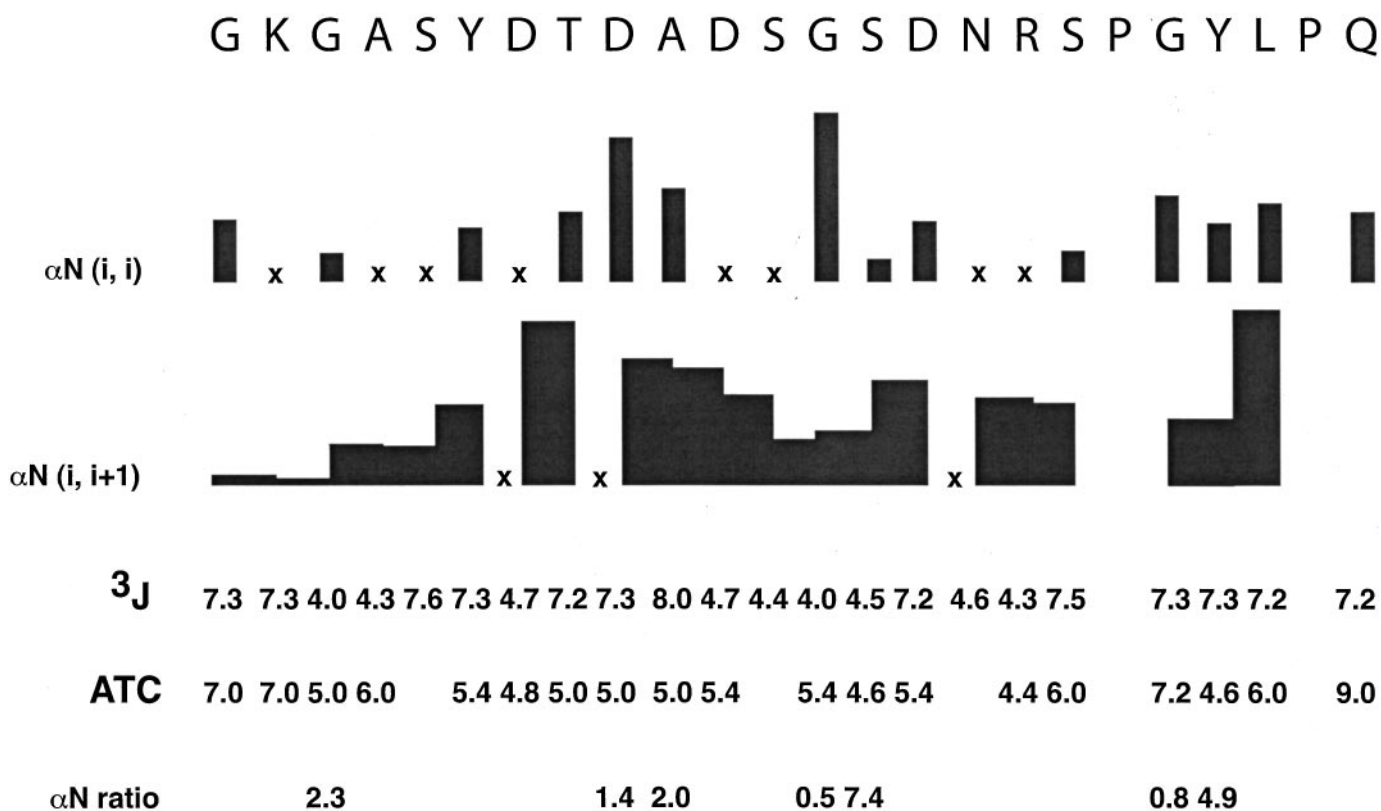


Figure 2. Summary of NMR parameters for Lustrin A D4 peptide in 1 mM Na₂HPO₄, 90% water/10% D₂O, 278 K pH 7.4. Refer to Figure 1 legend for explanation of terms.

in an extended conformation with no significant shielding of backbone amide (NH) protons from solvent exchange [13–15]. Thus, we conclude that both Lustrin A domains do not adopt α -helix or β -sheet structure; rather, they appear to exist largely in a conformationally labile random coil state or, in the case of RKSY, in a random coil state that is in conformational exchange with an extended state.

SEM Analysis of In Vitro Calcite Overgrowth Assays

Direct investigations of polypeptide interactions with aragonite are difficult to pursue, owing to the fact that aragonite is thermodynamically unstable in solution (i.e., transforms to calcite) [16, 17]. Thus, we must rely on indirect assessments such as the in vitro {104} geologic calcite epitaxial overgrowth assay [16, 17] as a “generic” qualitative probe of polypeptide interactions with crystalline calcium carbonates in general. The {104} cleavage plane of calcite features exposed carbonate and Ca (II) atoms [16, 17] and thus represents a putative interface for protein carboxylate Ca (II) and/or Arg, Gln, Lys, Tyr, Ser-carbonate interactions. Previous geologic overgrowth assay studies indicate that strong affinity for the calcium carbonate can significantly alter the overgrowth morphology and/or interrupt crystal nucleation [16–18]. Using the geologic calcite overgrowth assay, we tested the Lustrin A RKSY, D4, and bovine serum albumin polypeptides for their ability to interact and inhibit calcium carbonate overgrowth in vitro, and, compared these results to those obtained in the absence of polypeptides (Figure 3).

As shown in Figure 3A, the negative control (no polypeptide) exhibited {104} overgrowth features typical rhombohedral step edges in regions undergoing apposition (white arrows), with confluent overgrowth appearing in all other regions. Compared with the negative control, overgrowth in the presence of bovine serum albumin (BSA, Figure 3B) is equally confluent, but does exhibit voids or fenestrations in the {104} thin film layer. These effects were found to be concentration-dependent, and most likely arise from nonspecific interactions between the BSA protein and the nucleating calcite interface. The nonspecific interactions and noninhibitory activity of serum albumin have been noted in other calcite nucleation studies [23], where it was proposed that the rigid structure of the albumin protein limits its adsorption onto the calcite surface. Our findings are similar, in that we do not observe cessation or interruption of the epitaxial growth layer in the presence of BSA. Overgrowth in the presence of the RKSY polypeptide (Figure 3C) did not exhibit interruption over the range of 6.7×10^{-9} to 3.3×10^{-7} M concentration; the epitaxial overgrowth was confluent, extensive, and no significant morphological changes were observed. In the limited regions where growth step formation was detected, the step edges appear rhombohedral and well defined (white arrow, Figure 3C). *The most dramatic morphological changes in calcite overgrowth nucleation were observed in the presence of the D4 24 mer polypeptide* (Figure 3D, 3E). In the presence of 6.7×10^{-9} M D4, the {104} overgrowth layer was observed to be extensive; however, in regions where growth

step formation was identified, the step edges appeared slightly rounded (Figure 3D). At 1.7×10^{-7} M D4 concentration, limited overgrowth was observed compared with negative controls (Figure 3E). Moreover, the edges of the overgrowth layer displayed nonrhombohedral, rounded edges clearly indicating that nucleation inhibition occurred. In the presence of 3.3×10^{-7} M D4, calcite overgrowth was completely inhibited (data not shown).

As we have described in this report, the 24-AA D4 and 30-AA RKSY domains adopt solution state conformations that are consistent with random coil or, in the case of RKSY, random coil in equilibrium with extended conformations. These conformers appear to be labile, and would be expected to adopt open structures in solution that would permit sidechain accessibility to exposed calcium carbonate mineral surfaces. Similar results were noted for the calcite-binding protein lithostathine, in which X-ray diffraction studies revealed that the mineral binding N-terminal domain adopts an extended conformation, which may be only one of several energetically stable conformations in solution [23]. The results of the in vitro calcite overgrowth assay indicate that the RKSY sequence does not display concentration-dependent, high-affinity interactions with calcium carbonates (Figure 3). However, it is clear that the D4 domain is capable of high-affinity interactions with calcium carbonates (Figure 3), indicating that of the two domains examined, D4, and not RKSY, is most likely a putative mineral interaction site for Lustrin A-calcium carbonate binding. Although our experiments are not specific for aragonite per se; these findings are consistent with the data obtained for the mineral-binding, random coil N-terminal domain, EEAQTELPQAR, of the pancreatic calcite-binding protein, lithostathine [23]. Here, N-terminal polypeptide interactions with the {104} plane required the predominant participation of carboxylate residues (Glu), with only minor participation of positively charged residues, such as Arg, and hydrogen-bonding donor/acceptor residues Thr and Gln; and a globally extended backbone structure [23].

Note that the D4 domain sequence contains 4 Asp residues as well as Tyr, Ser, Arg, Lys, Asn, and Gln residues [1], which correlate with its demonstrated ability to interact with calcium carbonates in vitro. Since RKSY possesses only “basic” residues, it is likely that the absence of Asp, Glu residues in the sequence of this domain severely limit this polypeptide’s ability to bind to calcium carbonates in vitro. It is likely that RKSY performs some function other than mineral binding within the Lustrin A protein; for example, it is plausible to suggest that Lustrin A, via the RKSY domain, interacts with one or more of these matrix components. Alternatively, we note the structural and sequence similarities between the RKSY domain and another extensible domain, i.e., the polyproline Type II-PEVK domain of titin [22]. Thus, it is also plausible that the RKSY domain evolved as an extensible domain that behaves as an entropic spring under force extension. Obviously, further experimental studies are required to resolve these issues.

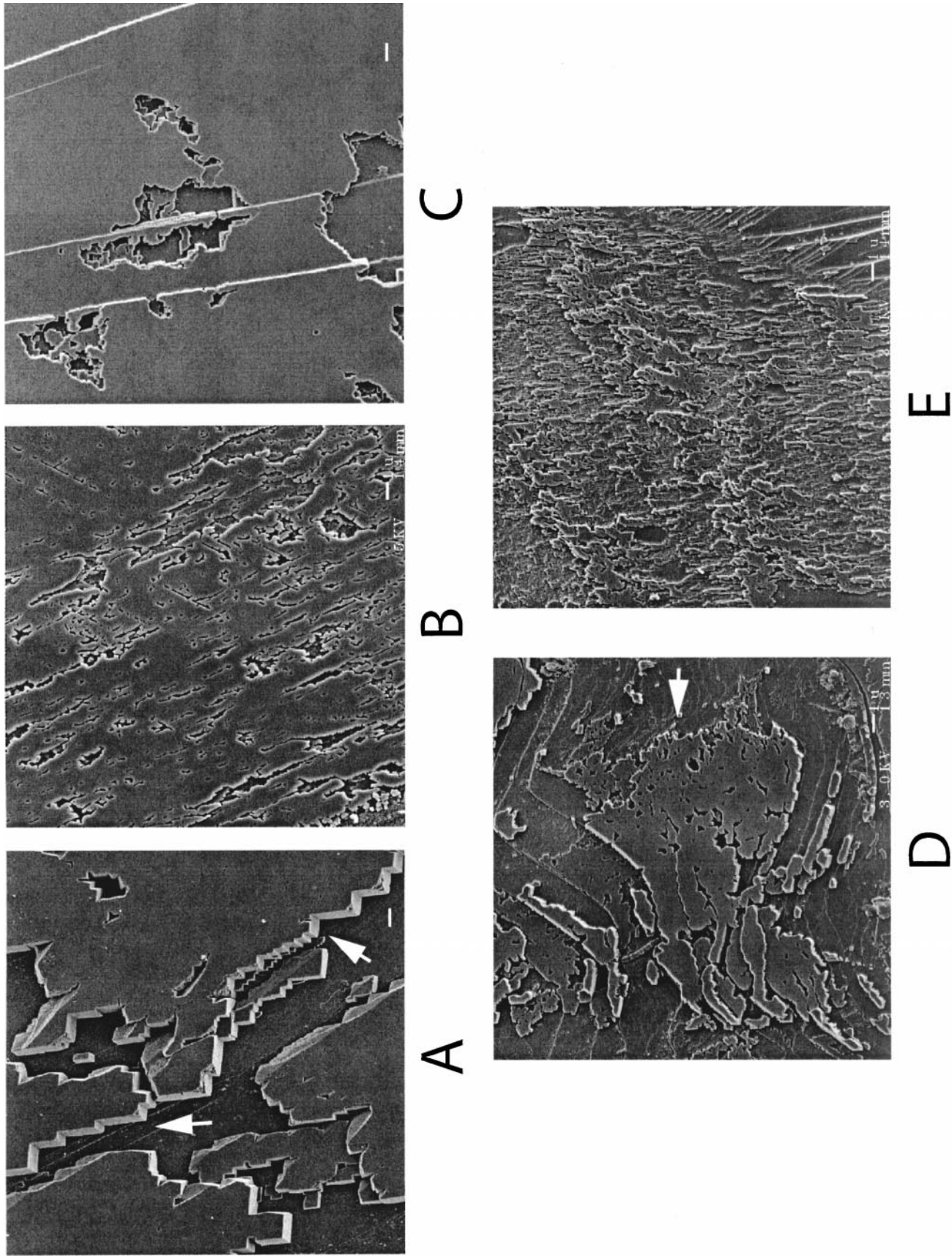


Figure 3. Scanning electron micrographs of calcium carbonate overgrowth on the {104} cleavage plane of geological calcite. (A) Negative control (no peptide added). Arrows indicate characteristic rhombohedral growth steps. In B–E the overgrowth nucleation was observed in the presence of (B) 3.3×10^{-8} M bovine serum albumin; (C) 1.7×10^{-7} M RKS Y polypeptide; (D) 6.7×10^{-9} M D4 polypeptide; and (E) 1.7×10^{-7} M D4 polypeptide. Scalebars in A–E-1 μm .

ACKNOWLEDGMENTS

Support for this study has been made possible by grants from the National Science Foundation (DMR 99-01356, MCB 98-16703 to NYU) and the Army Research Office (MURIDAAH04-96-1-0443 to UCSB).

REFERENCES

- [1] Shen, X., Belcher, A.M., Hansma, P.K., Stucky, G.D., and Morse, D.E. (1997). Molecular cloning and characterization of Lustrin A, a matrix protein from shell and pearl nacre of *Haliothis rufescens*. *J. Biol. Chem.* 272:32472–32481.
- [2] Smith, B.L., Schaffer, T.E., Viani, M., Thompson, J.B., Frederick, N.A., Kindt, J., Belcher, A., Stucky, G.D., Morse, D.E., and Hansma, P.K. (1999). Molecular mechanistic origin of the toughness of natural adhesives, fibers, and composites. *Nature* 399:761–763.
- [3] Lowenstam, H.A., and Weiner, S. (1989). In *On Biomineralization*, pp. 1–30 (New York: Oxford University Press).
- [4] Zhang, B., Wustman, B., Morse, D., and Evans, J.S. (2002). Model peptide studies of sequence regions in the elastomeric biomineralization protein, Lustrin A. I. The C-domain consensus-PG-, -NVNCT-motif. *Biopolymers* 63:358–369.
- [5] Schulz, G.E. (1991). Domain motions in proteins. *Curr. Opin. Struct. Biol.* 1:883–888.
- [6] Kempner, E.S. (1993). Movable lobes and flexible loops in proteins. *FEBS Lett.* 326:4–10.
- [7] Xu, G., and Evans, J.S. (1996). The application of “excitation sculpting” in the construction of selective one-dimensional homonuclear coherence transfer experiments. *J. Magn. Reson. Series B* 111:183–185.
- [8] Callahan, D., West, J., Kumar, S., Schweitzer, B.I., and Logan, T.M. (1996). Simple, distortion-free homonuclear spectra of peptides and nucleic acids in water using excitation sculpting. *J. Magn. Reson. Series B* 112:82–85.
- [9] Stott, K., Stonehouse, J., Keeler, J., Hwang, T.-L., and Shaka, A.J. (1995). Excitation sculpting in high-resolution nuclear magnetic resonance spectroscopy. Application to selective NOE experiments. *J. Am. Chem. Soc.* 117:4199–4200.
- [10] Meissner, A., Duus, J.O., and Sorensen, O.W. (1997). Spin-state-selective excitation. Application for E. COSY measurement of J_{HH} coupling constants. *J. Magn. Reson.* 128:92–97.
- [11] Xu, G., Zhang, B., and Evans, J.S. (1999). PFG ω_1 -filtered TOCSY experiments for the determination of long-range heteronuclear and homonuclear coupling constants and estimation of J-coupling “crosstalk” artifacts in 2-D ω_1 filtered “E.COSY-Style” spectra. *J. Magn. Reson.* 138:127–134.
- [12] Griesinger, C., Sorensen, O.W., and Ernst, R.R. (1987). Practical aspects of the E. COSY technique. Measurement of scalar spin-spin coupling constants in peptides. *J. Magn. Reson.* 75:474–492.
- [13] Xu, G., and Evans, J.S. (1999). Model peptide studies of sequence repeats derived from the intracrystalline biomineralization protein, SM50. I. GVGGR and GMGGQ repeats. *Biopolymers* 49:303–312.
- [14] Zhang, B., Xu, G., and Evans, J.S. (2000). Model peptide studies of sequence repeats derived from the intracrystalline biomineralization protein, SM50. II. Pro, Asn-rich tandem repeats. *Biopolymers*, 54:464–475.
- [15] Andersen, N.H., Neidigh, J.W., Harris, S.M., Lee, G.M., Liu, Z., and Tong, H. (1997). Extracting information from the temperature gradients of polypeptide NH chemical shifts. I. The importance of conformational averaging. *J. Am. Chem. Soc.* 119:8547–8561.
- [16] Walters, D.A., Smith, B.L., Belcher, A.M., Stucky, G.D., Morse, D.E., and Hansma, P.K. (1997). Modification of calcite growth by abalone shell proteins: An atomic force microscope study. *Biophys. J.* 72:1425–1433.
- [17] Thompson, J.B., Palocz, G.T., Kindt, J.H., Michenfelder, M., Smith, B.L., Stucky, G., Morse, D.E., and Hansma, P.K. (2000). Direct observation of the transition from calcite to aragonite growth as induced by abalone shell proteins. *Biophys J.* 79:3307–3312.
- [18] Michenfelder, M., Thompson, J., Shimizu, K., Le, K., Smith, B.L., Weaver, J., Lawrence, C., Stucky, G., Hansma, P., and Morse, D. Characterization of two crystal-modulating proteins isolated from the gastropod mollusc, *Biopolymers*, in press.
- [19] Feibig, K.M., Schwalbe, H., Buck, M., Smith, L.J., Dobson, C.M. (1996). Towards a description of the conformations of denatured states of proteins. Comparison of a random coil model with NMR measurements. *J. Phys. Chem.* 100:2661–2666.
- [20] Neri, D., Billiter, M., Wider, G., Wuthrich, K. (1992). NMR determination of residual structure in a urea-denatured protein, the 434 repressor. *Science* 257:1559–1563.
- [21] Logan, T.M., Theriault, Y., Fesik, S.W. (1994). Structural characterization of the FK506 binding protein unfolded in urea and guanidine hydrochloride. *J. Mol. Biol.* 236:637–648.
- [22] Ma, K., Kan, L.S., and Wang, S. (2001). Polyproline II helix is a key structural motif of the elastic PEVK segment of titin. *Biochemistry* 40:3427–3438.
- [23] Gerbaud, V., Pignol, D., Loret, E., Bertrand, J.A., Berlandi, Y., Fontecilla-Camps, J.C., Canselier, J.P., Gabas, N., and Verdier, J.M. (2000). Mechanism of calcite crystal growth inhibition by the N-terminal undecapeptide of lithostathine. *J. Biol. Chem.* 275:1057–1064.